Available online at www.sciencedirect.com
SCIENCE DIRECT®
Computer Aided Geometric Design 21 (2004) 353–369
COMPUTER AIDED GEOMETRIC DESIGN
www.elsevier.com/locate/cagd

Mesh quality improvement and other properties in the four-triangles longest-edge partition

Ángel Plaza [a,*], José P. Suárez [b], Miguel A. Padrón [c], Sergio Falcón [a], Daniel Amieiro [a]

[a] *Department of Mathematics, University of Las Palmas de Gran Canaria, Spain*
[b] *Department of Cartography and Graphic Engineering, University of Las Palmas de Gran Canaria, Spain*
[c] *Department of Civil Engineering, University of Las Palmas de Gran Canaria, Spain*

Received 21 January 2003; received in revised form 17 December 2003; accepted 14 January 2004

Abstract

The four-triangles longest-edge (4T-LE) partition of a triangle t is obtained by joining the midpoint of the longest edge of t to the opposite vertex and to the midpoints of the two remaining edges. The so-called self-improvement property of the refinement algorithm based on the 4-triangles longest-edge partition is discussed and delimited by studying the number of dissimilar triangles arising from the 4T-LE partition of an initial triangle and its successors. In addition, some geometrical properties such as the number of triangles in each similarity class per mesh level and new bounds on the maximum of the smallest angles and on the second largest angles are deduced.

Keywords: Refinement; Longest-edge based algorithms; Mesh quality; Similarity classes

1. Introduction

Modern CAD/CAM systems allow user to access specific application programs for different tasks such as finite/boundary element meshing for analysis, geometric calculation by integrals, and rendering objects on a graphical display. These application programs use to operate on approximate piecewise lower order representations of the exact geometry under study and then mesh modeling plays a major role in such systems.

For real-time visualization of NURBS surfaces, meshing algorithms are needed since they are utilized by the actual graphics hardware through the conversion to triangle meshes. Meshes are easily obtained from physical objects through scanning and reconstruction (Bertram et al., 2000). They also

* Corresponding author.
E-mail address: aplaza@dmat.ulpgc.es (Á. Plaza).

0167-8396/$ – see front matter
doi:10.1016/j.cagd.2004.01.001

provide hierarchical representations that can be used to generate Level of Details (LOD) or progressive representations (Hoppe, 1996; Luebke, 2001). Meshes can be refined to smooth surfaces through subdivision (Rassineus et al., 2003).

In the context of finite element method, adaptivity of the mesh and the analysis of the approximation error are important issues to be addressed (Carey, 1997). In recent years many partitions and associated refinement and coarsening algorithms have been proposed and studied. In the area of adaptive finite element methods, mesh refinement algorithms that maintain the *non-degeneracy* of the elements and the *conformity* and *smoothness* of the grid are certainly desirable. Non-degeneracy means that the minimum angle of the triangles is bounded away from zero when the partition or the refinement is applied. Conformity refers to the requirement that the intersection of nondisjoint triangles is either a common vertex or a common edge. The smoothness condition states that the transition between small and large elements should be gradual.

Non-degeneracy, conformity and smoothness are also desirable properties in adaptive tessellation of NURBS surfaces (Kumar, 2000). In this sense, Delaunay meshes have been widely used since they avoid long and skinny triangles and produce the maximum possible smallest-internal angle of any triangle (Bern and Eppstein, 1995). Refinement techniques are also used for enhancement of mesh obtained from trimmed NURBS surfaces, see an application in (Rabi Kumar et al., 2001). The number of triangles can be further increased/decreased depending on the application requirement.

Longest-edge based algorithms have been used with Delaunay triangulation for the quality triangulation problem (Hitschfeld et al., 2003; Rivara et al., 2001), and even the fractal properties of the meshes obtained by these algorithms have been pointed out in (Bova and Carey, 1992).

Some bisection based refinement methods have had exact angle counts since they first existed (Arnold et al., 2000; Bänch, 1991; Maubach, 1995; Mitchell, 1992) and consequently the non-degeneracy of the triangulation is proved. However, the 4 triangles longest-edge (4T-LE) refinement algorithm proposed by Rivara (1984) is missing an exact count of the similarity classes generated. Based on a theorem from Rosenberg and Stenger (1975), Rivara shows that arbitrary repetition of her algorithm never produces an angle smaller than half the minimum original angle. In practice, Rivara refinement typically improves angles (Bern and Eppstein, 1995), but this improvement has not been studied in depth so far. The issue is of interest in order to discriminate whether an initial mesh is good enough depending on the expected improvement to be produced when the 4T-LE partition is iteratively applied.

In this paper we study and delimit the self-improvement property of the 4T-LE partition, as a consequence of a sharp counting and numbering of the different triangles obtained by this partition. In addition, we look at the bonus bound on the evolution of the angles and other geometric properties.

2. 4-triangle longest-edge partition. Statement of the problem

Definition 1. The longest-edge (LE) partition of a triangle t_0 is obtained by joining the midpoint of the longest edge of t_0 with the opposite vertex (Fig. 1(a)). The 4-triangles longest-edge (4T-LE) partition is obtained by joining the midpoint of the longest edge to the opposite vertex and to the midpoints of the two remaining edges (see Fig. 1(b)).

As in (Rivara and Iribarren, 1996), for any triangle t, its edges and angles will be respectively denoted in decreasing order $r_1 \geqslant r_2 \geqslant r_3$, and $\gamma \geqslant \beta \geqslant \alpha$. Furthermore, $t(\alpha, \beta, \gamma)$ will be the class of similar

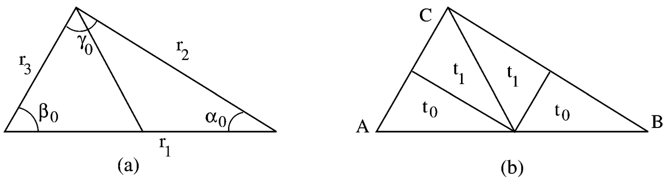

Fig. 1. (a) LE partition of triangle t_0, (b) 4T-LE partition of triangle t_0.

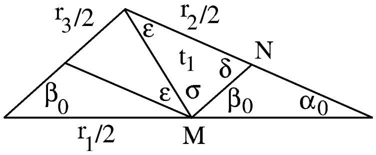

Fig. 2. Notation for the new angles.

triangles of angles $\gamma \geqslant \beta \geqslant \alpha$. Interchangeably, t will represent an element of the class $t \in t(\alpha, \beta, \gamma)$ or the class itself.

Since the first 4-triangles longest-edge partition of any triangle t_0 introduces two new edges parallel to the edges of t_0, the following result holds (Rivara and Iribarren, 1996):

Proposition 2. (a) *The first 4-triangles longest-edge partition of a single triangle t_0 produces two triangles similar to t_0 and two* (*potentially*) *new similar triangles t_1 which we will call second generation triangles.* (b) *The iterative 4-triangles longest-edge partition of any triangle t_0 introduces* (*at most*) *one new dissimilar triangle per iteration.*

2.1. Statement of the problem

How many dissimilar triangles can be generated by the repeated application of the 4T-LE partition to an initial triangle? The answer to this question depends on the geometry of the initial triangle, as can be clearly seen after a few trials. The problem is equivalent to discovering under what conditions the application of the 4T-LE partition no longer generates new dissimilar triangles, and in how many applications of the 4T-LE partition these conditions are fulfilled.

Call ε, σ, and δ the angles of the second generation triangle t_1, and M and N the midpoints of the longest and second longest edge as in Fig. 2. Considering that $|MN| = r_3/2 \leqslant r_2/2$, then $\varepsilon \leqslant \sigma$. Therefore the largest angle can only be either δ, or σ. Besides, if δ is the largest angle of the three angles, then the opposite edge is the longest one of the triangle t_1 and so, the generation of new dissimilar triangles stops. So, the problem is simply to determine when $\delta \geqslant \sigma$ in the partitioning process. Note that for all the acute initial triangles t_0, $\delta \geqslant \sigma$, while for right triangles only triangles similar to the initial one are generated. Hence, we will mainly consider obtuse triangles throughout the remainder of this paper, if no explicit indication is given on the contrary.

3. Number of similarity classes. New bounds and exact number

Let us recall initially the following results from Rivara and Iribarren (1996).

Theorem 3. *Let t_0 be an initial obtuse triangle in which the 4T-LE partition is iteratively applied. Then a (finite) sequence of dissimilar triangles, one per iteration, is obtained*: $\{t_0, t_1, t_2, \ldots, t_N, t_{N+1}\}$, *where triangles $t_0, t_1, t_2, \ldots, t_{N-1}$ are obtuse, triangle t_N is not obtuse, and the 4T-LE partition of t_N produces (at most) a new obtuse triangle t_{N+1}. And at this point no new dissimilar triangles are produced.*

The iterative 4-triangles longest-edge partition produces a finite sequence of 'better' triangles satisfying the properties illustrated in Diagram 1 (Rivara and Iribarren, 1996) until triangle t_N becomes nonobtuse,

$$\begin{array}{ccccccc}
t_0 & \to & t_1 & \to & t_2 & \to \cdots \to & t_N \\
\text{(obtuse)} & & \text{(obtuse)} & & \text{(obtuse)} & & \text{(nonobtuse)} \\
\alpha_0 & & \alpha_1 > \alpha_0 & & \alpha_2 > \alpha_1 & & \alpha_N > \alpha_{N-1} \\
\gamma_0 & & \gamma_1 \leqslant \gamma_0 - \alpha_1 & & \gamma_2 \leqslant \gamma_1 - \alpha_2 & & \gamma_N \leqslant \gamma_{N-1} - \alpha_N
\end{array}$$

Diagram 1.

where α_i and γ_i are respectively the smallest and the largest angles of triangle t_i. The arrow emanating from triangle t_i to triangle t_{i+1} means that the (first) 4-triangles longest-edge partition of triangle t_i produces the new dissimilar triangle t_{i+1}.

The process described in the preceding diagram inevitably results in one of the situations illustrated in Diagram 2 (Rivara and Iribarren, 1996):

$$\begin{array}{llllllll}
(1) & t_{N-1} & \rightleftharpoons & t_N & & & \gamma_{N-1} + \gamma_N = \pi \\
 & \text{obtuse} & & \text{nonobtuse} & & & \\
(2) & t_{N-1} & \to & t_N \circlearrowleft & & & \gamma_N = \pi/2 \\
 & \text{obtuse} & & \text{right-angled} & & & \\
(3) & t_{N-1} & \to & t_N & \rightleftharpoons & t_{N+1} & \gamma_N + \gamma_{N+1} = \pi \\
 & \text{obtuse} & & \text{nonobtuse} & & \text{obtuse} &
\end{array}$$

Diagram 2.

Rivara and Iribarren also give an upper bound for the number of dissimilar triangles generated:

Theorem 4. *For any initial obtuse triangle t_0, the number K of dissimilar triangles generated throughout the process is bounded as follows*

$$K \leqslant \left\lceil \frac{\gamma_0 - \frac{\pi}{3}}{\alpha_0} \right\rceil + 1. \tag{1}$$

3.1. Improvement of the previous bound

Theorem 5. *The number of dissimilar triangles that appear in the repeated application of the 4T-LE partition to an initial triangle t_0, say K, satisfies*

$$\begin{cases} K = 2 & \text{if } \gamma_0 < \frac{\pi}{2}, \\ K = 1 & \text{if } \gamma_0 = \frac{\pi}{2}, \\ K \leqslant \left\lfloor \left| \frac{\gamma_0 - \pi/2}{\alpha_0} \right| \right\rfloor + 2 & \text{if } \gamma_0 > \frac{\pi}{2}. \end{cases} \tag{2}$$

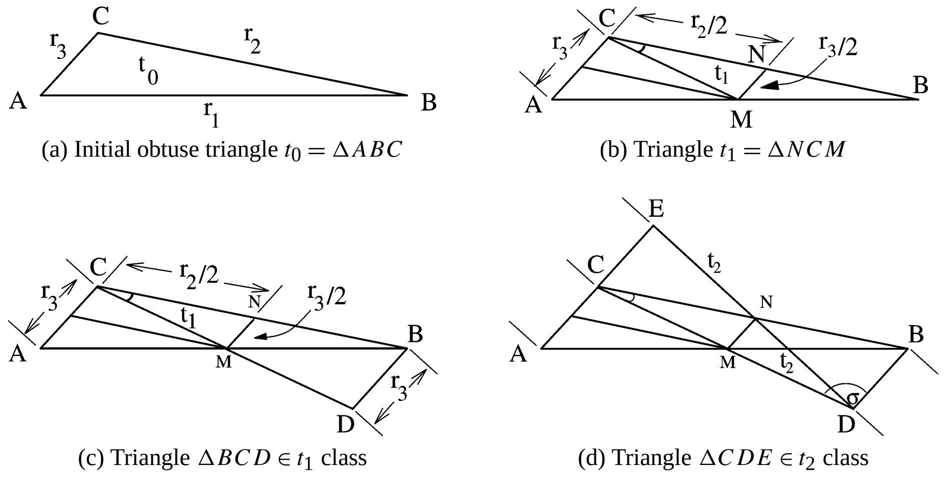

Fig. 3. Original triangle t_0 and new dissimilar triangles t_1 and t_2.

Proof. Note that while the new triangle t_j is obtuse then $\gamma_j < \gamma_0 - j\alpha_0$ for $j = 1, 2, \ldots, N-1$. Since γ_j is the largest angle of the obtuse triangle t_j, $\gamma_j > \frac{\pi}{2}$, so $\frac{\pi}{2} < \gamma_j \leqslant \gamma_0 - j\alpha_0$, which implies that

$$j \leqslant \frac{\gamma_0 - \pi/2}{\alpha_0}.$$

Considering that in the sequence $\{t_0, t_1, t_2, \ldots, t_N, t_{N+1}\}$, triangles $t_0, t_1, t_2, \ldots, t_{N-1}$ are obtuse, $\gamma_j > \frac{\pi}{2}$ for $j = 1, 2, \ldots, N-1$, we get the result. □

Although the new computed bound is better than the previous one, for obtuse triangles with the smallest angle near zero, this bound is still very far from the actual number of dissimilar triangles generated.

3.2. New bounds for the number of similarity classes

Here we first present a new lower bound for the number of dissimilar triangles generated by the 4T-LE partition. The geometric idea developed in Figs. 3 and 4 will provide us with a lower bound. The idea is then used to obtain a quasi-exact upper bound. Finally, we offer a simple procedure for the exact number of triangles.

Lemma 6. *The number of dissimilar triangles, K, arising in the iterative application of the 4T-LE partition to an initial triangle $t_0 = t_0(\alpha_0, \beta_0, \gamma_0)$, is bounded from below as follows*:

$$\left\lceil \frac{\cos\beta_0 \sin\gamma_0}{\sin\alpha_0} \right\rceil \leqslant K. \tag{3}$$

Proof. First, consider an initial (obtuse) triangle $\Delta ABC = t_0(\alpha_0, \beta_0, \gamma_0)$ as in Fig. 3(a).

By applying the 4T-LE partition to t_0, a new dissimilar triangle $t_1(\alpha_1, \beta_1, \gamma_1) = \Delta NCM$ is obtained as in Fig. 3(b). For this new triangle t_1 we construct point D, by translating point M by vector $\overrightarrow{CM}$, so $D = M + \overrightarrow{CM}$. Then, by joining point D with point B a new triangle ΔBCD appears as in Fig. 3(c).

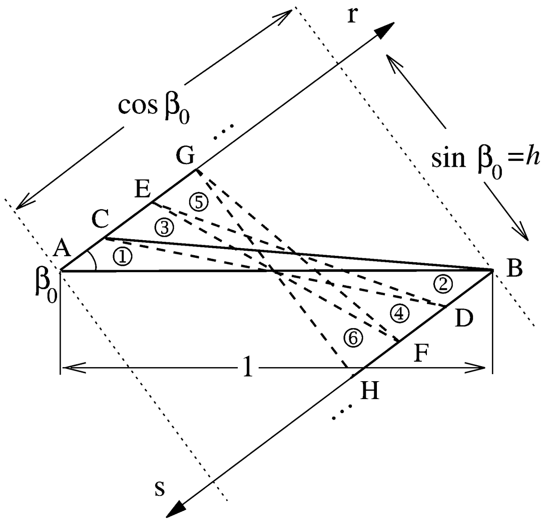

Fig. 4. Sequence of dissimilar triangles generated by the 4T-LE partition. The longest-edge of the initial triangle has been normalized to length 1.

Note that triangle ΔBCD is similar to t_1 because they share angle at vertex C and the edges of t_1 CM and CN are half of the corresponding edges CD and CB of ΔBCD. So $\Delta BCD \in t_1(\alpha_1, \beta_1, \gamma_1)$. Now, if the application of the 4T-LE partition to triangle ΔBCD does not generate a new dissimilar triangle, then the largest angle of ΔBCD is at B. Otherwise, the largest angle is at D. In this last case, by applying the same process to triangle ΔBCD a new dissimilar triangle $t_2 = \Delta CDE$ is obtained, Fig. 3(d). Points A, C, and E are equally spaced and lie on a straight line.

Note, that while the triangles obtained before are obtuse, the application of the 4T-LE partition produces a new dissimilar triangle (as in Fig. 4). Furthermore, all the triangles obtained are obtuse at the latest vertex. For example, triangle ΔABC is obtuse at C, triangle ΔBCD is obtuse at D, etc., until the last nonobtuse triangle is generated (triangle ΔFGH in Fig. 4).

In Fig. 4 the initial triangle has been normalized since it has the longest edge equal to 1. Then, by the law of sines, the shortest edge AC, is of length $|AC| = \frac{\sin\alpha_0}{\sin\gamma_0}$ and the height of this triangle over the base AC is $h = \sin\beta_0$. Figure 4 shows all the triangles between two parallel straight lines r and s. All the triangles have the same height $h = \sin\beta_0$ and the associated bases the same length, $|AC| = |BD| = |CE| = |DF| = |EG| = |FH|$.

All the triangles are obtuse while the height h falls outside the opposite edge, and in all of them the obtuse angle is in the last vertex. But, for the first triangle in which the height falls inside the opposite edge (ΔFGH in Fig. 4), this triangle is acute or obtuse in the vertex immediately before to the last one (vertex G in triangle ΔFGH of Fig. 4). Now the number of triangles generated is at least equal to the number of divisions of the segment $\cos\beta_0$ in Fig. 4 by the shortest edge of the initial triangle, edge AC, in Fig. 4. □

Remark 7. The last triangle obtained via the previous process:

(1) either is nonobtuse (acute or right) as in Fig. 4, or

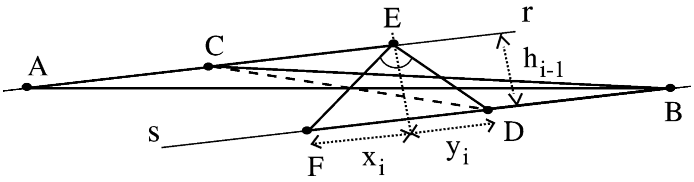

(a) Triangles between lines r and s

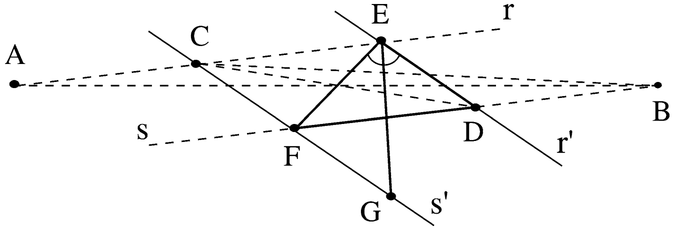

(b) New triangles between lines r' and s'

Fig. 5. New generation of triangles if triangle ΔDEF is obtuse in E.

(2) is obtuse on the opposite vertex to the only edge on one of the lines r and s, as can be seen in Fig. 5(a). In this case, the same process can be applied with this newly created triangle as in Fig. 5(b).

The previous lemma and remark allow us to give a simple procedure for obtaining an upper bound of the number of dissimilar triangles generated:

Theorem 8. *The number of dissimilar triangles arising from the application of the 4T-LE partition to any initial triangle t_0 and its successors is upper bounded by U, with U given by the following algorithm*:

Upper bound algorithm (t_0, U)
/ Input variables*: t_0, *initial triangle*
/ Output variables*: *upper bound of number of dissimilar triangles U*
/ Let $\alpha_0 < \beta_0 < \gamma_0$ the angles of t_0*, $\phi_i = \frac{\cos\beta_i \sin\gamma_i}{\sin\alpha_i}$
$U = 1$; $i = 0$
while $\gamma_i > \frac{\pi}{2}$ **do**
  $U = U + \lceil\phi_i\rceil - 1$
  $h_i = \sin\beta_i$
  $x_i = \max\{\lceil\phi_i\rceil - \phi_i,\ \phi_i - \lfloor\phi_i\rfloor\}$
  $y_i = \min\{\lceil\phi_i\rceil - \phi_i,\ \phi_i - \lfloor\phi_i\rfloor\}$
  $x_i = x_i \frac{\sin\alpha_i}{\sin\gamma_i}$
  $y_i = y_i \frac{\sin\alpha_i}{\sin\gamma_i}$
  $i = i + 1$
  / The angles of the last triangle are computed*
  $\alpha_i = \arctan\frac{h_{(i-1)}}{x_{(i-1)}}$
  $\beta_i = \arctan\frac{h_{(i-1)}}{y_{(i-1)}}$

$\gamma_i = \pi - \alpha_i - \beta_i$
end while
$U = U + 1$
end

Proof. This algorithm takes into account the possibility that the last triangle generated between the two parallel lines r and s may be acute or obtuse (see Figs. 4 and 5). The angle in this vertex is acute in Fig. 4 but obtuse in Fig. 5. In the second case, the last triangle plays the role of the initial triangle for which the same process is applied. For this case see Fig. 5. The (finite) sequences of dissimilar triangles generated can be written as in Diagram 3, where at the right, the number of dissimilar triangles generated is calculated. Since the last triangle of each sub-sequence is the first triangle of the next sub-sequence, $U = U - 1 + \lceil \phi_j \rceil$, with $2 \leqslant j \leqslant k + 1$:

$$\begin{array}{l|l}
\{t_0, t_1, \ldots, t_{\lceil \phi_0 \rceil - 1} = t_1^1, & U = \lceil \phi_0 \rceil \\
\;t_1^1, t_2^1, \ldots, t_{\lceil \phi_1 \rceil}^1 = t_1^2, & U = U - 1 + \lceil \phi_1 \rceil \\
\;t_1^2, t_2^2, \ldots, t_{\lceil \phi_2 \rceil}^2 = t_1^3, & U = U - 1 + \lceil \phi_2 \rceil \\
\quad \vdots & \quad \vdots \\
\;t_1^k, t_2^k, \ldots, t_{\lceil \phi_k \rceil}^k \} & U = U - 1 + \lceil \phi_k \rceil
\end{array}$$

Diagram 3.

In this way, we have a loop which ends when the last triangle ($t_{\lceil \phi_k \rceil}^k$) is not obtuse. Note that since $\frac{\pi}{2} \leqslant \gamma_N \leqslant \gamma_0 - N\alpha_1$, then

$$N \leqslant \left\lfloor \frac{\gamma_0 - \pi/2}{\alpha_0} \right\rfloor.$$

In addition, $\lceil \phi_k \rceil \geqslant 1$, and hence the number of loops, $k + 1$ verifies

$$k + 1 \leqslant \frac{N}{\min(\phi_i)} \leqslant \left\lfloor \frac{\gamma_0 - \frac{\pi}{2}}{\alpha_0} \right\rfloor$$

and the algorithm always ends. Finally, since the partition of an acute triangle by means of the 4T-LE partition gives at most one more triangle, the upper bound U is obtained. □

3.3. Exact number of triangles

Theorem 9. *Let t_0 be an initial triangle, and let K be the exact number of dissimilar triangles generated by the 4T-LE partition when this partition is applied to t_0 and its descendants. Then K can be calculated as follows*:

Exact number algorithm (t_0, K)
Upper bound (t_0, U)
/* *Let $\alpha < \beta < \gamma$ the angles of the last triangle computed*
if $\gamma \geqslant \beta$, **then**
  if $\gamma = \frac{\pi}{2}$, **then** $K = U - 1$

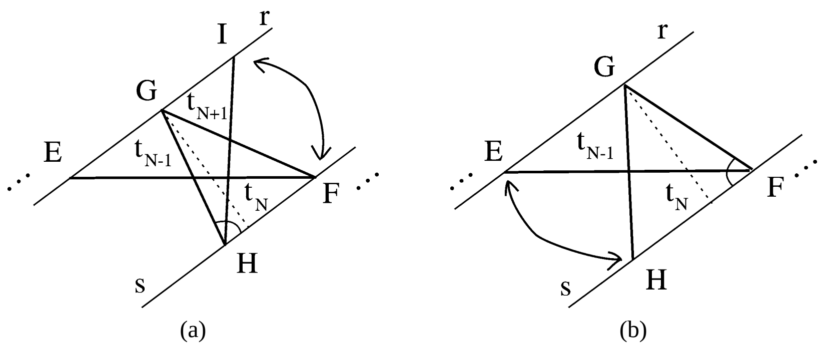

Fig. 6. Two different situations after generating a nonobtuse triangle t_N: (a) One more dissimilar obtuse triangle appears, (b) no more different triangles are generated.

else $K = U$
end if
else
$\delta = \begin{cases} 1 & \textit{if } \phi_i - \lfloor \phi_i \rfloor \leqslant 0.5, \\ 0 & \textit{otherwise} \end{cases}$
$K = U - \delta$
end if
end

Once the first nonobtuse triangle, t_N, is obtained, two possible situations are distinguished: either by dividing this triangle by the 4T-LE partition we get an obtuse triangle similar to another previous triangle, or a new obtuse triangle t_{N+1} is obtained. See Fig. 6. In the figure triangle t_N is not obtuse, while the new triangle t_{N-1} is obtuse. In Fig. 6(a) one more dissimilar triangle t_{N+1} appears, while in Fig. 6(b) no more dissimilar triangles are generated since $t_{N+1} = t_{N-1}$. This issue is equivalent to the decimal part of $\frac{\cos\beta_0 \sin\gamma_0}{\sin\alpha_0}$, as the theorem claims.

4. Number of triangles on each similarity class

In this Section, we study the number of triangles belonging to each similarity class, when the 4T-LE partition is repeatedly applied on any initial (obtuse) triangle and its successors.

Proposition 10. *Let $\tau_0 = \{t_0\}$ be an initial triangular mesh with only one* (*obtuse*) *triangle t_0. Suppose that by the 4T-LE partition $k+1$ classes of triangles are generated and let $\Gamma = \{\tau_0, \tau_1, \ldots, \tau_k, \ldots, \tau_n, \ldots\}$ be the* (*infinite*) *sequence of nested meshes obtained by uniform application of 4T-LE partition to the previous mesh. Then, the number of elements of similarity class t_j at mesh level τ_m, $t_j^{(m)}$ verifies*

$$t_j^{(m)} = \begin{cases} 2^m \binom{m}{j} & \textit{for } j \leqslant k-2, \\ \frac{1}{2}\left[4^m - 2^m \sum_{j=0}^{k-2} \binom{m}{j} + 2^m \binom{m-1}{k-2}\right] & \textit{for } j = k-1, \\ \frac{1}{2}\left[4^m - 2^m \sum_{j=0}^{k-2} \binom{m}{j} - 2^m \binom{m-1}{k-2}\right] & \textit{for } j = k. \end{cases} \tag{4}$$

Table 1
Evolution of number of triangle-class per mesh level

Ref.	t_0	t_1	t_2	$\cdots$	t_{k-1}	t_k
τ_0	1					
τ_1	2	2				
τ_2	4	8	4			
$\vdots$	$\vdots$	$\vdots$	$\vdots$	$\ddots$		
τ_{k-1}	$t_0^{(k-1)}$	$t_1^{(k-1)}$	$t_2^{(k-1)}$	$\cdots$	$t_{k-1}^{(k-1)}$	
τ_k	$t_0^{(k)}$	$t_1^{(k)}$	$t_2^{(k)}$	$\cdots$	$t_{k-1}^{(k)}$	$t_k^{(k)}$
$\vdots$	$\vdots$	$\vdots$	$\vdots$	$\vdots$	$\vdots$	$\vdots$
τ_n	$t_0^{(n)}$	$t_1^{(n)}$	$t_2^{(n)}$	$\cdots$	$t_{k-1}^{(n)}$	$t_k^{(n)}$
$\vdots$	$\vdots$	$\vdots$	$\vdots$	$\vdots$	$\vdots$	$\vdots$

Proof. Since the 4T-LE partition divides each triangle in four, the number of generated triangles in the n stage of refinement is $T_n = 4^n$. Let us write the number of triangles of similarity class t_j in the n stage of refinement, $t_j^{(n)}$, in matrix form as in Table 1.

The elements belonging to the first $k-1$ columns (that is $j \leqslant k-2$) verify the relation $t_j^{(m)} = 2t_j^{(m-1)} + 2t_{j-1}^{(m-1)}$, so, taking into account the initial condition $t_0^{(0)} = 1$ and the properties of the binomial coefficients (Graham et al., 1989) we get

$$t_j^{(m)} = 2^m \binom{m}{j} \quad \text{for } 0 \leqslant j \leqslant k-2. \tag{5}$$

On the other hand, the iterative 4T-LE partition of any obtuse triangle t_0 produces a finite sequence of dissimilar triangles, $t_j^{(i)}$, $0 < j \leqslant k$. After that, no new dissimilar triangles are generated. Moreover, from a t_k triangle two triangles t_{k-1} and two triangles t_k are obtained, and from a t_{k-1} triangle two triangles t_{k-1} and two triangles t_k are also obtained, so for $k-1 \leqslant j \leqslant k$ we get

$$\begin{aligned} t_{k-1}^{(m)} &= 2t_{k-2}^{(m-1)} + 2t_{k-1}^{(m-1)} + 2t_k^{(m-1)}, \\ t_k^{(m)} &= 2t_{k-1}^{(m-1)} + 2t_k^{(m-1)}. \end{aligned} \tag{6}$$

From (5), $t_{k-2}^{(m-1)} = 2^{m-1}\binom{m-1}{k-2}$, so $t_{k-1}^{(m)} = 2^m\binom{m-1}{k-2} + t_k^{(m)}$. Finally, since

$$T_m = 4^m = \sum_{j=0}^{k} t_j^{(m)} = \sum_{j=0}^{k-2} 2^m \binom{m}{j} + 2^m \binom{m-1}{k-2} + 2t_k^{(m)}, \tag{7}$$

we get the conclusion. □

It should be noted that terms $t_{k-1}^{(m)}$ and $t_k^{(m)}$ can also be expressed as hypergeometric functions but do not admit a closed formula since they involve partial sums of binomial coefficients weighted, in this case, by the exponential coefficient 2^m (Graham et al., 1989).

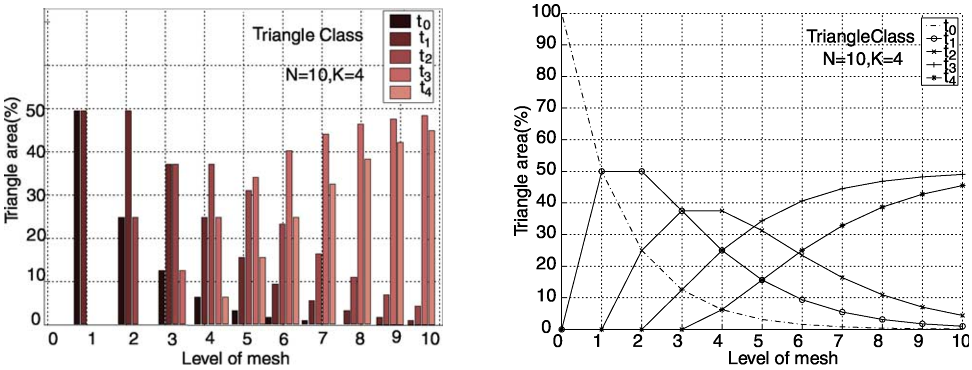

(a) Area covered (%) per mesh level

(b) Evolution of classes of triangles

Fig. 7. Distribution of different classes of triangles.

Corollary 11. *In the situation of previous proposition the number of elements of similarity class t_j at mesh level τ_m, $t_j^{(m)}$ verifies*

$$\lim_{m\to\infty} \frac{t_j^{(m)}}{4^m} = \begin{cases} 0 & \text{for } j \leqslant k-2, \\ \frac{1}{2} & \text{for } j = k-1, k. \end{cases} \tag{8}$$

Figure 7 shows the evolution of the relative numbers of triangles in each similarity class when the 4T-LE partition proceeds iteratively in an initial triangle t_0 and its successors, in complete agreement with Corollary 11.

5. Results about the minimum and second largest angles

Corollary 12. *Let t_0 be an initial (obtuse) triangle. Let $\{t_0, t_1, \ldots, t_N\}$ be the (finite) sequence of dissimilar triangles generated by the repeatedly application of the 4T-LE partition, where t_N is the first nonobtuse triangle. Let $\{\alpha_0, \alpha_1, \ldots, \alpha_N\}$ be the sequence of smallest angles. Let α_{MAX} be the largest of the smallest angles generated throughout the process. Then, $\alpha_{\mathrm{MAX}} = \alpha_N$, and α_{MAX} can be bounded depending on the values of the initial angles as follows*:

$$\begin{cases} \arctan\left(\dfrac{\sin\alpha_0}{\sin\gamma_0 \sin\beta_0}\right) \leqslant \alpha_{\mathrm{MAX}}, \\ \text{if} \quad \dfrac{\sin\alpha_0}{\sin\gamma_0} \leqslant \sin\beta_0, \quad \alpha_{\mathrm{MAX}} \leqslant 2\arctan\left(\dfrac{\sin\alpha_0}{2\sin\gamma_0\sin\beta_0}\right). \end{cases} \tag{9}$$

Proof. Let us again consider Fig. 4. There, all the new dissimilar triangles are drawn, except the obtuse triangle that appears from dividing the last (nonobtuse) triangle (triangle ΔFGH in Fig. 4). In the figure, the triangles have the same area, and their shortest edges have same length. In the hypothesis of $\frac{\sin\alpha_0}{\sin\gamma_0} \leqslant \sin\beta_0$, then all the triangles generated through the 4T-LE partition satisfy that their height over the shortest edge is equal to $\sin\beta_0$, after normalizing all the triangles to having the same height over the shortest edge, as shown in Fig. 4. Therefore, the two possibilities for the best and worst situations in the smallest angles generated are as depicted in Fig. 8. □

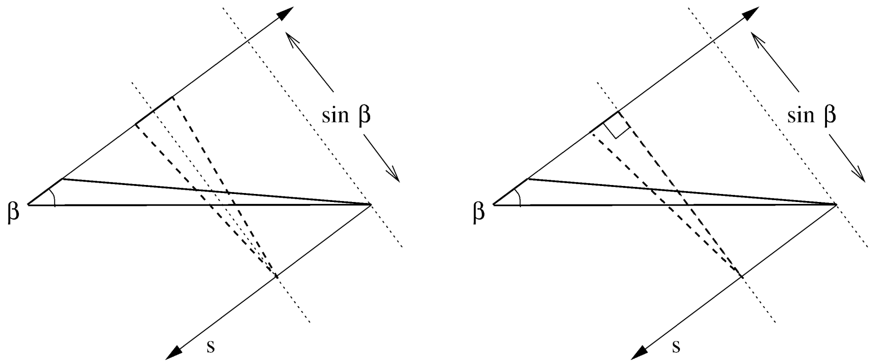

(a) The last triangle is isosceles (b) The last triangle is right

Fig. 8. Situations in which the maximum (a) and lower (b) bounds of the maximum of the minimum angle are respectively achieved.

The last corollary gives a lower bound of the maximum of the minimum angle generated throughout the application of the 4T-LE partition to an initial triangle t_0, thus it gives a lower bound of the *max–min angle condition*. These last two conditions emphasize how much an initial triangulation may improve by global application of the 4-triangles longest-edge partition. For a lower bound of the smallest angle, $\alpha_{\min}$ (*min–min condition*) generated it is known the lower bound: $\frac{\alpha_0}{2} \leqslant \alpha_{\min}$ (Rosenberg and Stenger, 1975), but this bound can be improved in the sense of the following corollary:

Corollary 13. *In the hypothesis of the previous corollary,* $\alpha_{\min} = \min\{\alpha_0, \frac{\alpha_N}{2}\}$*, where, as before, angle* α_N *is the smallest angle of the first nonobtuse triangle obtained.*

Now we shall prove a result of the behavior of the second largest angles when the 4T-LE partition is applied to any obtuse triangle t_0.

Corollary 14. *Let* t_0 *be any initial obtuse triangle with angles* α_0, β_0, *and* γ_0 *such that* $\alpha_0 < \beta_0 < \frac{\pi}{2} < \gamma_0$. *Suppose that the 4T-LE partition is iteratively applied on* t_0 *producing a (finite) sequence of dissimilar triangles* $\{t_i\}$, *with angles* α_i, β_i, *and* γ_i $(\alpha_i < \beta_i < \gamma_i)$. *Consider the sequence of dissimilar triangles* $\{t_0, t_1, \ldots, t_N\}$ *generated, where* t_N *is the first nonobtuse triangle. Then, the respective sequence of second largest angles* $\{\beta_0, \beta_1, \ldots, \beta_N\}$ *is an increasing sequence.*

It should be noted that this result was conjectured by Rivara and Iribarren (1996) after experimental observation, although they did not provide any proof.

Proof. It is sufficient to consider two consecutive triangles as in Fig. 9.

In the figure, two triangles with vertices ABC and BCD appear. Triangle ΔBCD has been obtained by 4T-LE partition of triangle ΔABC. The second largest angles are noted in the figure as β_0 and β_1, respectively. Now, since $\tan(\beta_0) = \frac{h}{x}$ and $\tan(\beta_1) = \frac{h}{y}$, and $y < x$ we have that $\tan(\beta_0) < \tan(\beta_1)$, and as $\beta_i < \frac{\pi}{2}$ we get $\beta_0 < \beta_1$. □

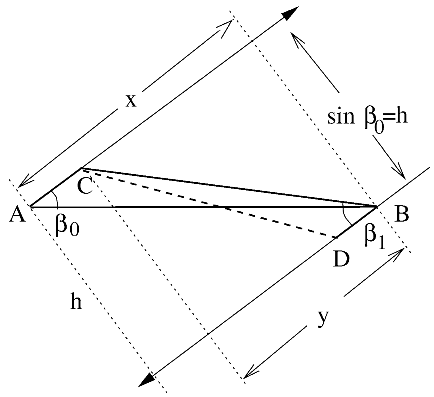

Fig. 9. Evolution of the second largest angles.

Corollary 15. *In the conditions of the previous corollary the second largest angles* $\{\beta_0, \beta_1, \ldots, \beta_N\}$ *are upper bounded by the expression*

$$\beta_i \leqslant \arctan\left(\frac{\sin\beta_0 \sin\gamma_0}{\sin\alpha_0}\right). \tag{10}$$

Proof. It is sufficient to consider Fig. 9 and the values of $h = \sin\beta_0$, and that $y \geqslant |AC| = \frac{\sin\alpha_0}{\sin\gamma_0}$, so

$$\tan\beta_i = \frac{h}{y} \leqslant \frac{\sin\beta_0}{\left(\frac{\sin\alpha_0}{\sin\gamma_0}\right)}. \qquad \square$$

Note that the upper bound for the second largest angles generated through the process of successive 4T-LE partitions is valid only while the triangles are obtuse. See Table 5 in the section of numerical examples. In the table, the first values of the second largest angles for the test triangles examples (β_0) appear, the values of the maximum second largest angles of the obtuse triangles generated (β_{MAX}), and finally the values of the upper bound (U_{Bound}).

6. Numerical examples

In this section we present some test triangles also studied by Rivara and Iribarren (1996) to compare the results presented by Rivara and Iribarren with the new bound, and the new sharp bound of the number of dissimilar triangles generated by the 4-triangles longest-edge partition. These numerical test problems are in complete agreement with the bounds and exact number presented before.

Table 2 shows four test triangles and the different shaped triangles obtained by the 4T-LE partition. In Table 3 we have added the values for the computed bounds on the number of similarity classes. In the table, RI means inequality (1). *Improved bound* stands for the upper bound in inequality (2), and *quasi-exact number* refers to the upper bound given by Theorem 8. In all the cases the procedure of Theorem 9 gives the exact number of dissimilar triangles that are generated by the 4T-LE partition.

Table 2
Sequences of dissimilar triangles obtained by the 4T-LE partition

It. n	Triangle 1 # of dissimilar triangles 15			Triangle 2 # of dissimilar triangles 11		
	γ_n	β_n	α_n	γ_n	β_n	α_n
0	145.455	32.595	1.950	173.972	5.423	0.605
1	143.292	34.545	2.164	173.216	6.028	0.756
2	140.885	36.708	2.407	172.245	6.784	0.971
3	138.200	39.115	2.684	170.952	7.755	1.293
4	135.202	41.800	2.998	169.148	9.048	1.804
5	131.850	44.798	3.351	166.462	10.852	2.686
6	128.107	48.150	3.743	162.066	13.538	4.396
7	123.937	51.893	4.170	153.735	17.934	8.331
8	119.316	56.063	4.621	133.923	26.265	19.812
9	114.235	60.684	5.081	84.274	49.648	46.077
10	108.715	65.765	5.520	95.726	43.599	40.676
11	102.811	71.285	5.904	84.274	49.648	46.077
12	96.618	77.189	6.193			
13	90.266	83.382	6.352			
14	89.734	83.907	6.359			
15	90.266	83.382	6.352			
It. n	Triangle 3 # of dissimilar triangles 8			Triangle 4 # of dissimilar triangles 4		
	γ_n	β_n	α_n	γ_n	β_n	α_n
0	169.900	8.572	1.527	114.624	54.900	10.475
1	167.721	10.100	2.180	102.073	65.376	12.551
2	164.371	12.279	3.349	88.250	77.927	13.824
3	158.625	15.629	5.747	91.750	74.623	13.627
4	146.921	21.375	11.704	88.250	77.927	13.824
5	117.268	33.079	29.652			
6	63.237	62.732	54.031			
7	116.763	33.270	29.967			
8	63.237	62.732	54.031			

On the other hand, Table 4 shows the lower and upper bounds of the largest of the smallest angles generated by the 4T-LE partition in the test examples. It should be noted here that Triangle 2 in Table 4 presents an $L_{\mathrm{Bound}} = 46.077$. Notice that this is not contrary to Corollary 17 since Triangle 2 does not satisfy the hypothesis required: $\frac{\sin\alpha_0}{\sin\gamma_0} \leqslant \sin\beta_0$.

Finally, Table 5 gives the initial value of the second largest angle (β_0) for each test triangle, the maximum value of the second largest angle generated while the triangle is obtuse (β_{MAX}) and the value given for the upper bound studied here.

For a better understanding of the auto-improvement property of the 4T-LE partition and the limits of this property as given in this paper, the successive triangles obtained have been transformed to share the longest edge, as is explained in Fig. 10. The different triangles obtained in the first test problem have been depicted in Fig. 11.

Table 3
Different bounds in the number of dissimilar triangles obtained

Triangle 1			Triangle 2		
γ_0	β_0	α_0	γ_0	β_0	α_0
145.455	32.595	1.950	173.972	5.423	0.605
Previous RI bound		45	Previous RI bound		190
Improved bound		30	Improved bound		140
Quasi-exact bound		**16**	Quasi-exact bound		**11**
# of dissimilar triangles		15	# of dissimilar triangles		11
Triangle 3			Triangle 4		
γ_0	β_0	α_0	γ_0	β_0	α_0
169.900	8.572	1.527	114.624	54.900	10.475
Previous RI bound		73	Previous RI bound		7
Improved bound		54	Improved bound		4
Quasi-exact bound		**8**	Quasi-exact bound		**4**
# of dissimilar triangles		8	# of dissimilar triangles		4

Table 4
Lower and upper bound for the largest smallest angles generated

Triangle 1				Triangle 2			
α_0	L_{Bound}	α_{MAX}	U_{Bound}	α_0	L_{Bound}	α_{MAX}	U_{Bound}
1.950	6.356	6.359	6.376	0.605	46.774	46.077	56.022
Triangle 3				Triangle 4			
α_0	L_{Bound}	α_{MAX}	U_{Bound}	α_0	L_{Bound}	α_{MAX}	U_{Bound}
1.527	45.553	54.031	54.032	10.475	13.736	13.824	13.937

Table 5
Upper bound for the second largest angles generated

Triangle 1			Triangle 2		
β_0	β_{MAX}	U_{Bound}	β_0	β_{MAX}	U_{Bound}
32.595	77.189	83.644	5.423	26.265	43.226
Triangle 3			Triangle 4		
β_0	β_{MAX}	U_{Bound}	β_0	β_{MAX}	U_{Bound}
8.572	33.079	44.450	54.900	65.276	76.263

7. Conclusions

In this paper the so-called *self-improvement* property of the 4-triangles longest-edge partition and the associated local refinement have been delimited. The quality of the triangles generated may improve but only within certain limits as has been found here.

Moreover, the problem of calculating the number of similarity classes of triangles generated by application of the 4-triangles longest-edge partition has been solved. Not only has the upper bound of the

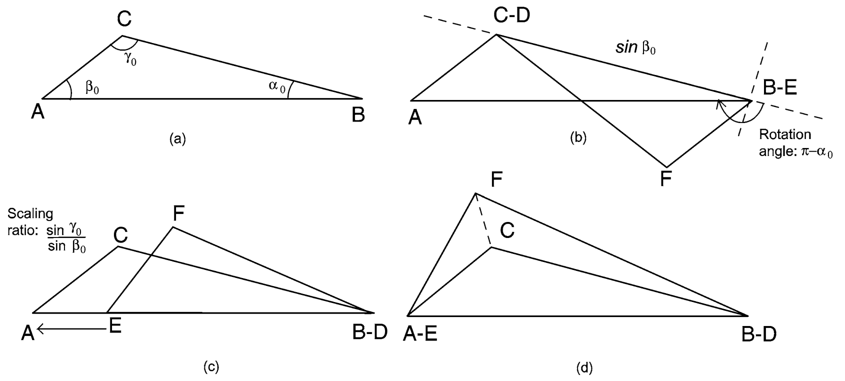

Fig. 10. Triangle DEF in (b) is transformed to share the same longest edge with triangle ABC in (d).

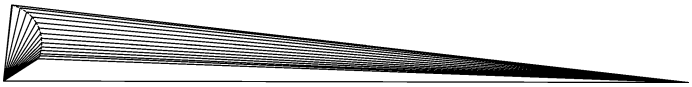

(a) Triangles normalized sharing the same longest edge

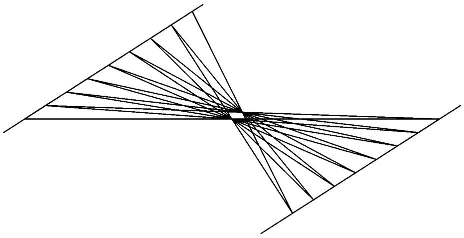

(b) Triangles normalized sharing the height

Fig. 11. Evolution of dissimilar triangles of example test 1.

number of dissimilar triangles generated been substantially improved, but also a simple procedure has been presented which allows for the exact number to be obtain.

In addition, the number of triangles in each similarity class has been mathematically studied, together with the distribution of the classes in each mesh level, whilst the new bounds on the smallest and second largest angles have been provided.

References

Arnold, D.N., Mukherjee, A., Pouly, L., 2000. Locally adapted tetrahedral meshes using bisection. SIAM J. Sci. Comput. 22 (2), 431–448.

Bänch, E., 1991. Local mesh refinement in 2 and 3 dimensions. IMPACT Comput. Sci. Engrg. 3, 181–191.

Bern, M., Eppstein, D., 1995. Mesh generation and optimal triangulation. In: Du, D.-Z., Hawang, F.K. (Eds.), Computing in Euclidean Geometry, second ed.. World Scientific, pp. 47–123.

Bertram, M., Barnes, J.C., Hamann, B., Joy, K.I., Pottmann, J., Wushour, D., 2000. Piecewise optimal triangulation for the approximation of scattered data in the plane. Comput. Aided Geom. Design 17 (8), 767–787.

Bova, S.W., Carey, G.F., 1992. Mesh generation/refinement using fractal concepts and iterated function systems. Internat. J. Numer. Methods Engrg. 33, 287–305.

Carey, G.F., 1997. Computational Grids: Generation, Refinement and Solution Strategies. Taylor and Francis.

Graham, R.L., Knuth, D.E., Patashnik, O., 1989. Concrete Mathematics. Addison-Wesley.

Hitschfeld, N., Villablanca, L., Krause, J., Rivara, M.-C., 2003. Improving the quality of meshes for the simulation of semiconductor devices using Lepp-based algorithms. Internat. J. Numer. Methods Engrg. 58, 333–347.

Hoppe, H., 1996. Progressive meshes. ACM SIGGRAPH 30, 99–108.

Kumar, S., 2000. Robust incremental polygon triangulation for fast surface rendering. J. WSCG 8 (1).

Luebke, D.P., 2001. A developer's survey of polygonal simplification. IEEE Comput. Graphics Appl. 21 (3), 24–35.

Maubach, J.M., 1995. Local bisection refinement for n-simplicial grids generated by reflection. SIAM J. Sci. Statist. Comput. 16 (1), 210–227.

Mitchell, W.F., 1992. Optimal multilevel iterative methods for adaptive grids. SIAM J. Sci. Statist. Comput. 13, 146–167.

Rabi Kumar, G.V.V., Srinivasan, P., Shastry, K.G., Prakash, B.G., 2001. Geometry based triangulation of multiple trimmed NURBS surfaces. Comput. Aided Design 33, 439–454.

Rassineus, A., Breitkopf, P., Villon, P., 2003. Simultaneous surface and tetrahedron mesh adaptation using mesh-free techniques. Internat. J. Numer. Methods Engrg. 57, 371–389.

Rivara, M.-C., 1984. Algorithms for refining triangular grids suitable for adaptive and multigrid techniques. Internat. J. Numer. Methods Engrg. 20, 745–756.

Rivara, M.-C., Iribarren, G., 1996. The 4-triangles longest-side partition of triangles and linear refinement algorithms. Math. Comp. 65 (216), 1485–1502.

Rivara, M.-C., Hitschfeld, N., Simpson, B., 2001. Terminal-edges Delaunay (small-angle based) algorithm for the quality triangulation problem. Comput. Aided Design 33, 263–273.

Rosenberg, I., Stenger, F., 1975. A lower bound on the angles of triangles constructed by bisecting the longest side. Math. Comp. 29, 390–395.